# Application of computational tools for the designing of Oleuropein loaded nanostructured lipid carrier for brain targeting through nasal route

Sucharitha Palagati [1,2] · Satyanarayana SV [3] · Bhaskar Reddy Kesavan [4]

## Abstract

**Purpose** Meningitis is an inflammation of meninges encircled the brain and spinal cord. Currently it can be treated with second generation cephalosporins which were ended up with an unresolvable problem called Multi Drug Resistance (MDR). Hence, there is a need to develop a better herbal molecule to conflict the MDR.

**Methods** Hot Blanching technique followed by ultra sound assisted extraction using bio-solvent aqueous glycerol was used to extract OLE from olive leaves. QbD tool was applied to predict the interactions between Critical Material Attributes (Ratio of solid Lipid $X_1$, Concentration of Surfactant $X_2$) and Critical Process Parameters (Homogenization Time $X_3$) on Critical Quality Attributes (CQA, Particle Size $Y_1$, Zeta Potential $Y_2$, and Entrapment Efficiency $Y_3$). Particulate characteristics were evaluated and Invivo pharmacokinetic study was done in albino Wistar rats by IV and IN route of administration.

**Results** Thermal studies reflect the formation of low ordered crystalline structure of lipid matrix which offers higher encapsulation of drug in NLC than physical mixture. CMA and CPP show significant effect on CQA and method operable design range was developed. Histo-pathological studies confirms that there is no signs of toxicity and in-vitro drug release studies reveals a rapid release of a drug initially followed by prolonged release of oleuropein upto 24 h. The absolute bioavailability of drug loaded NLC in brain was higher in IN route compared to NLC administered by IV route.

**Conclusions** In a nutshell, challenges offered by the hydrophilic OLE for brain targeting can be minimized through lipidic nature of NLC.

**Keywords** Hot blanching · Bio-solvent · Oleuropein · QbD · Brain targetting

## Introduction

In the recent years, the prevalence of neurodegenerative disorders was emerging rapidly. Among them, Bacterial meningitis

✉ Sucharitha Palagati
sucharitha89pharma@gmail.com

1 Department of Pharmaceutics, Jawaharlal Nehru Technological University Anantapur, Ananthapuramu, Andhra Pradesh 515001, India

2 Department of Pharmaceutics, Sri Venkateswara College of Pharmacy, RVS Nagar, Chittoor, Andhra Pradesh 517127, India

3 Department of Chemical Engineering, Jawaharlal Nehru Technological University Anantapur, Ananthapuramu, Andhra Pradesh 515001, India

4 Department of Pharmaceutics, Centre for Nanotechnology, Sri Venkateswara College of Pharmacy, Chittoor, Andhra Pradesh 517127, India

is the foremost one affecting approximately 4 million people around the country and this prevalence is expected to upswing a maximum of 10 million by 2030. Many strategies have been chalked out to alleviate the prevalence of meningitis. But, the physiological protective barriers around the brain made them inefficient and most challenging. Hence, new treatment modalities are in pipeline to overcome these challenge [1].

Currently, various invasive and non- invasive methods were established for brain targeting of hydrophilic and lipophilic moieties to brain. Out of all, a promising approach i.e., nose to brain targeting of a drug moiety is most attractive way which unveils a big challenge of drug delivery to brain through BBB [2]. Loading of drug into a suitable colloidal carrier system is a pre-requisite to achieve a therapeutic efficacy from drug molecule. Hence, in the current research NLC was selected to circumvent the fundamental limitations of brain targeting and intranasal delivery i.e., limited therapeutic concentrations and mucociliary Clearance of drug [3, 4]. Tailoring of NLC with herbal moiety "Oleuropein" extracted from olive leaves was

framed to advent the targeting potential of thiscarrier system for brain targeting through nasal delivery [5].

Oleuropein demonstrates all the pre-requisite characters that make it suitable candidate for development of intra-nasal NLC. It offers limited solubility in water and other organic solvents; possess extensive first pass hepatic metabolism, average bio-availability, low CSF concentration oral administration etc. In the development of NLC, especially during the loading of hydrophilic drug, it circumvents major challenges like solubility of drug in lipid matrix, entrapment efficiency and drug loading, uniformity of particle size, stability and poor drug targeting. Hence, in the current hypothesis a major focus was laid on maximizing the drug entrapment efficiency, site targeting and particle size through minimal trails [6].

To accomplish the hypothesis, the study was articulated like extraction, isolation and purification of Oleuropein, screening of lipids, and experimental design by QbD using JMP Software to establish a functional relationship between critical material attributes and critical process parameters (CMA's & CPP's) with critical quality attributes (CQA's), evaluation of particulate parameters by Dynamic Light Scattering (DLS), surface morphology by SEM and TEM, In-vivoPharmacokinetic studies and IVIVC [7].

To the point, in this work we engineered a hybrid Lipid Nanocarrier system based on QbD approach for nose to brain targeting of Oleuropein and the designed NLC's were further studied for its physicochemical, molecular, microstructural, ex-vivo permeation and stability aspects.

## Materials

Olive Leaves was purchased from Rajasthan Olive Cultivation Limited, Rajasthan. Tefose was gifted by Gattefose (Mumbai, India). Capmul was gifted by Abitec Corporation Ltd. (Mumbai, India). Polysorbate 80, Polaxomer 188, Sorbate 80 and MF Millipore membrane filters of 0.45 μm pore size was purchased from Merck, India. Dialysis tubing (Mol wt. 6000–8000 Da and flat width of 23 mm) was purchased from Sigma Aldrich (Bangalore, India). HPLC grade solvents were used for HPLC analysis and all other chemicals and reagents were of analytical grade.

## Methods

### Extraction of Oleuropein from olive leaves

Pre- treated Ultra Sound Assisted Extraction (UAE) of oleuropein (OLE) from olive leaves were performed by using Ultra Sonicator (Q Sonica Q800, 20KHZ). A measured weight of 30 g of powdered sample was mixed with Water: Glycerol (3:1) %v/v at a solvent ratio of 50 ml/g in a container. This mixture was sonicated at 300 W for about 10 min under

intermittency ratio, ∞ of 4/5. Where, ∞ - fraction of cycle; ∞ = ton/(ton +toff). After sonication, the menstrum was screened using fine cloth and concentrated using Rotary flash evaporator at 40 °C. The extract was dissolved in methanol, filtered by using 0.45 μ syringe filterprior to spectral studies [8].

### Fractionation and purification of olive leaf extract

Solid Phase extraction technique (SPE) was used for purification of extract. SPE was done by using super clean cartridges (LS-18, 20 ml, Germany) and 10 g of modified silica. The olive leaf extract (100 mg) was dissolved in 10 ml of water and loaded into cartridges. The extracts were eluted with methanol of various % v/v (0%, 10%, 20%, 30%, 40%, 50%, 60%, 70%, 80%, 90% and finally 100%). Fractions were collected and evaporated to dryness under vaccum at 40 °C in a Rotavapour and redissolved in methanol for further analysis. The compound Oleuropein was analyzed by HPLC Technique [9].

### Thermal studies

The thermal properties and phase transitions behavior of the drug, lipid blend, placebo, NLC, Physical mix were investigated by using DSC (DSC 60; Schimadzu, Tokyo, japan). DSC measurement were performed in a range of 10–190 °C at a heating rate at 10 °C/min to a temperature of 30 °C throughout the analysis using Indium as standard reference. Sample weight of about 2 mg was used in this study. Melting Point values were determined from the endothermic peak and Crystallinity index was estimated using Enthalpy of bulk material and enthalpy of NLC. The recrystallization index (RI) was computed by following equation [10].

$$\%RI = \frac{\Delta HNLC}{\Delta HBL \times Fraction\ of\ Lipid} \times 100$$

Where: $C$ = Enthalpy of NLC; $\Delta HBL$ = Enthalpy of lipid.

### Preparation of Oleuropein loaded NLC by melt-emulsification and ultrasonication

Oleuropein loaded NLC were prepared by melt-emulsification and ultrasonication method. Briefly, a mixture of Solid lipid (Tefose) and Liquid lipid (Capmul) was taken in a ratio of 60:40, melted 5 °C above the melting point of solid lipid. The drug: lipid ratio was maintained at 1.4%w/w and specified quantity of drug was dissolved in molten lipid with the aid of vortex until a clear solution was obtained. Surfactant (Polaxomer 188: Polysorbate 80: Soy Lecithin, 1:1:0.5) was added into aqueous solution and heat the solution upto the temperature of lipid blend. At this juncture, hot lipid phase was added to hot surfactant solution and subject this mixture to homogenization at 10000 RPM to attain a uniform lipid

blend of primary emulsion followed by ultrasonication for 10 min (30:5 on: off lych) to obtain NLC. The obtained NLC was allowed to cool at RT and characterized further. The % of aqueous phase was (95% by weight) and lipid phase was (5% by weight), Sodium azide (0.02%) was added to prevent microbial growth in NLC [11].

## Experimental design

Experimental study of Oleuropein loaded NLC was done with an objective to maximize the entrapment efficiency, minimize particle size with optimal ZP and PDI. After the preliminary understanding of important factors influencing the CQA, A 3 level Central Composite Design (CCRD) was chosen to explore the optimum levels of CMA and CPP on CQA. The CMA's and CPP's selected were Ratio of Lipid ($X_1$), Concentration of surfactant ($X_2$), Homogenization time ($X_3$), whereas critical quality attributes were Particle size ($Y_1$), Zeta Potential ($Y_2$), and Entrapment Efficiency ($Y_3$). The data were analyzed using JMP 13.0 Software, and the coded, actual values of resultant batches with their obtained responses were presented in Table 2 [12].

The statistical significance of each response was analyzed by using Pareto Chart as shown in the Fig. 2. t-values can be studied by two limit lines namely Bonferroni limit & t limit line. Qualitative and Quantitative contribution of each variable on the response was analyzed by JMP Software 13.0. Polynomial equation is used to validate the statistical design and the coded values are transformed into actual values by using principle of power transformation. The magnitude of correlation is expressed in terms of Polynomial equation which have either +ve sign indicates synergistic effect (or) −ve sign indicates antagonistic effect. The qualitative and quantitative relationship between CMA and CPP with CQA can be explained by 2D contour plots and 3D response plots. Best model was selected on the basis of CV, $R^2$, adjusted $R^2$ and check the validity of model [13].

## Desirability criteria

Desirability function (multi-response optimization technique) was applied and total desirability was calculated by using JMP software. The desirability ranges in between 0 and 1 represents the magnitude of closeness of response to its ideal value.

## Check point analysis

Check point analysis was done to confirm the utility of established contour plots and reduced polynomial equation in the formulation of OLE loaded NLC. Levels of material and process attributes were taken from three check points on contour plots plotted at fixed levels of −1,0,+1. The values of PS, ZP and EE were calculated by substituting the values in

polynomial equation. NLC were prepared experimentally on same check points and the difference of theoretically computed values of responses and experimental values was compared by using student-t test and % error was estimated.

## Characterization of NLC

### Particle size measurement (PS)

In order to predict the suitability of formulated NLC, particle size analysis was performed on the day of formulation. Dynamic Light scattering is a most widely used noninvasive technique to measure particle size and PDI based on electrophoretic mobility. Particle size of the formulated NLC's were measured at 25 °C by photon correlation spectroscopy (Dynamic light scattering) using Zetasizer (Horiba). The measurement was conducted after dilution of samples with distilled water upto a concentration of 0.1% w/w, to get suitable scattering intensity and to weaken the opalescence. The mean diameter and PDI values were estimated at an angle of 90° in 10 mm diameter cells at 25 °C [14].

### Zeta potential (ZP)

ZP was measured by using Zetasizer (Horiba). The samples were diluted with purified water and adjusting conductivity (50 μs/cm) with potassium chloride solution (0.1% w/v). The pH was in the range of 5.5–7.5. ZP was estimated from the electrophoretic mobility using Helmholtz Equation. Each sample was estimated 3 times and mean values and SD are represented [15].

### Determination of %EE and % drug loading

The %EE of OLE within NLC was measured by estimating the concentration of free drug in NLC dispersion. A measured volume of 20 ml NLC dispersion was diluted with distilled water and centrifuged at 25,000 rpm for 30 min at 25 °C to settle the colloidal nanoparticles. Supernatant was collected and the amount of free drug was estimated spectrophotometrically at 280 nm using HPLC [16]. % EE and % DL was calculated by following equation.

$$\%EE = \frac{Amount\ of\ Oleuropein\ added - Amount\ of\ Oleuropein\ in\ NLC}{Amount\ of\ Oleuropein\ added}$$

$$\%DL = \frac{Amount\ of\ Oleuropein\ added - Amount\ of\ Oleuropein\ in\ NLC}{Weight\ of\ NLC}$$

### Transmission electron microscopy (TEM)

The morphological features of OLE loaded NLC was observed by TEM (TEM 1200 Ex. Japan) using negative

staining method. NLC was diluted with distilled water and place a drop of sample on carbon coated copper grid. Excess of water were removed with filter paper and set aside for 10 min. After 10 min, a drop of 4% (w/v) solution of phosphofungtic at solution was added, allow it for 5 min to absorb and analyze the sample. Record the images at 120KV and 40,000X magnification [16].

### Scanning electron microscopy (SEM)

SEM images of Oleuropein loaded NLC were taken by depositing the drop of sample on stub using one end adhesive dried carbon tape (NEM, Tape, Japan). Working distance was maintained upto 35 mm and acceleration voltage used was 17KV with secondary electron image (SEI) as a detector [17].

### Invitro drug release studies

Invitro drug release from Oleuropein loaded NLC and pure drug OLE was carried out by dialysis bag method. NLC containing an equivalent amount of 100 mg of Oleuropein were dropped in pre-soaked dialysis bag of molecular weight cut off 12–14 KDa, both ends were tied and immersed in the phosphate buffered saline of pH 6.8 and volume of 500 ml upto 24 h at $37 \pm 0.1$ °C temperature. Samples were withdrawn at regular time intervals of 0.5, 1, 2, 3, 4, 5, 6, 8, 12, 16 and 24 h from receptor compartment and the same volume was replaced by fresh dissolution medium. Filter the samples with 0.45 μ filters and dilute them to a pre-requisite concentration with buffer. Absorbance was measured at 280 nm using HPLC by keeping placebo as blank. After cessation of drug release, cumulative amount of Oleuropein release was plotted as a function of time. Experiments were repeated 3 times and the results were expressed as mean values ± SD [18].

### Determination of nanoparticle induced hemolysis in blood

In-vitro hemolytic method was used to measure hemolysis by spectrophometic technique. 1 mg/ml of oleuropein loaded NLC was incubated in blood. Undamaged erythrocytes were screened and measure the absorbance at 540 nm. Same protocol was executed for fresh blood sample which are not incubated with NLC and hemolytic percentage (HP %) can be calculated using the following formula [19].

$$Hp\% = \frac{DT - DN}{DPC - DN} \times 100$$

Where, DT= Absorbance of test sample; DN= Absorbance of negative control; Dpc= Absorbance of positive control.

### Nasal histopathology

Histopathological examination was done on goat nasal mucosa to predict the pathological changes after the administration of NLC. Nasal mucosa having thickness of (0.3 mm) was selected four in number. Each nasal mucosa was treated with OLE solution in PBS pH 6.8 (24.5 mg/ml), Blank NLC, OLE NLC (equivalent to 24.5 mg of OLE), Isopropyl alcohol (Mucociliary toxic agent, +ve control) respectively for 1 h. After the treatment, nasal septum was fixed in 10% HCHO for 24 h, decalcified and washed with tap water and then dehydrated by ethanol. Paraffin blocks were prepared for sectioning by slide microtone of thickness 5 μm to embed the nasal mucosa. The tissue sections were collected on glass slides, deparaffinized and stained with Hematoxylin – eosin stains. Slides of treated and untreated tissue were observed under light microscope and examined by a pathologist blinded to experimental conditions [20–22].

## Invivo pharmacokinetic studies

### Selection criterion of Wistar rats

The guidelines of committee for the purpose of control and supervision on experimental animals (CPCSEA) were followed to design experimental protocol and it was approved by the ethical committee of Sri Venkateswara College of Pharmacy bearing approval No SVCOP/IAEC/005-2016-17. Invivo studies were functionalized with albino male Wistar rats of weight 180–200 g. Before the commencement of experimental process, allow the rat to acclimatize for temperature $(24 \pm 1$ °C) and humidity $(55 \pm 10\%)$. Rats were fed with standard pelletized diet and the health status of the rats was examined continuously throughout the process. Rats were divided into 4 groups and each group contains 6 animals [23].

### Administration of NLC to albino Wistar rats

Male Wistar rats weighing (200–250 g) were selected for this study. Animals were grouped into 4 batches and each group contains 6 animals. Group I was administered with vehicle, Group II with pure Oleuropein aqueous solution, Group III with Oleuropein NLC in IV route, Group IV with Oleuropein NLC in IN route at a dose of 1 mg/kg of body weight. Rats were anaesthetized with anesthetic ether before administration of the drug. IV administration was done through peripheral vein of the rat tail. For intranasal administration, instillation of NLC into the nasal cavity was done by using a polyethylene canula connected to a 100 μl micropipette. After the administration, blood samples were collected through cardiac puncture at an intervals of 5, 10, 20,30,45,60,120, 180 and 360 min. Collected blood samples were mixed with disodium EDTA to prevent clumping and centrifuge the blood samples

at 7000 rpm for 20minat 4 °C. Separate serum and plasma. Brains were decapitated with skulls cut, opened and tissue sample were isolated at different time points. Wash the brain tissue sample with normal saline, bottled drug with tissue paper and store at −80 °C until complete analysis [24–26].

### Plasma sample analysis

Standard solution of OLE was prepared by dissolving 5 mg of OLE with 8 ml of methanol (1000 ppm). Working standard was prepared from standard solutions with appropriate dilution using mobile phase. Plasma calibration standard were prepared by spiking the plasma concentration with OLE to 100 μl of standard plasma and sample, followed by 300 μl of mobile phase. Vortex the sample for 10 min and centrifuge it for about 15 min at 10000 rpm at 4 °C. Separate serum and plasma portions were collected and subject it to HPLC analysis.

### Brain tissue sample analysis

Blank brain tissue was homogenized with Oleuropein. Approximately 300 mg of test tissue was weighed and add 100 μl of internal standard followed by 1000 μl of methanol. Homogenize the sample for 5 min and centrifuged for about 15 min in 10,000 rpm at 4 °C. Supernatant were screened and subjected to HPLC analysis [27, 28].

$$Drug\ Targetting\ Efficiency\ (DTE\%) = \left\{ \frac{\left[\frac{(AUC)brain}{(AUC)blood}\right]IN}{\left[\frac{(AUC)brain}{(AUC)blood}\right]IV} \right\} \times 100$$

$$Drug\ Targetting\ Potential(DTP\%) = \frac{Bin-Bx}{Bin}$$

$$Bx = \frac{Bix}{Piv}Xin$$

Bx = AUC (Area Under Curve) blood brain fraction – internal standard; Biv = AUC blood fraction –IV; Bin = AUC (brain) – internal standard; Pin = AUC (blood) – internal standard.

### Invitro – Invivo correlation studies

The percentage of drug absorbed at specific time interval was estimated from the drug concentration data using Wagner – Nelson method and interpretation of data was done by using linear regression method.

### Data analysis

The mean concentration of Oleuropein in plasma and brain samples were obtained by plotted a pharmacokinetic graph (Time on X-axis, Plasma concentration of Y-axis). From the graph, Cmax, Tmax can be notified directly. AUC was

calculated by using Trapezoidal rule without extrapolation to 'α'. The remaining PK parameters, ke, MRT, Cl, V and $t_{1/2}$ for individual set of data were estimated according to PK solver software. During the whole process of study, weight of the animals was monitored daily at a fixed time and any signs of mortality and toxic effects were monitored.

## Results & discussion

### Isolation and purification of NLC

Solid Phase Extraction technique was majorly used for fractionation and purification of olive leaf extract. As shown in Table 1 and Fig. 1, 11 fractionates were collected and % concentration of drug "Oleuropein" was estimated quantitatively by using High Pressure Thin layer Chromatography (HPTLC).

### Thermal studies

DSC is a useful tool for the estimation of degree of Crystallinity, Polymorphism and incompatibility between drug and lipid. DSC thermograms of drug, lipids, Physical mixture and drug loaded NLC formulation were presented in Fig. 2. Oleuropein drug shows a sharp melting endothermic peak at 88.3 °C. The lipids show a slight pre-shift in the peak with a melting temperature ranging from 83 to 84 °C. Thermal analysis of Oleuropein loaded NLC was done after 7 days of production. No significant shift in the peak was observed in the physical mixture which indicates a good compatibility of drug and lipids. From the thermograms it was found that, no melting peak of OLE was detected for drug loaded NLC which indicates that drug was completely soluble in the lipid matrix. This finding was attributed due to change in crystal lattice of lipid during formulation of NLC and also small

**Table 1** Concentration of Oleuropein in fractionates by HPTLC

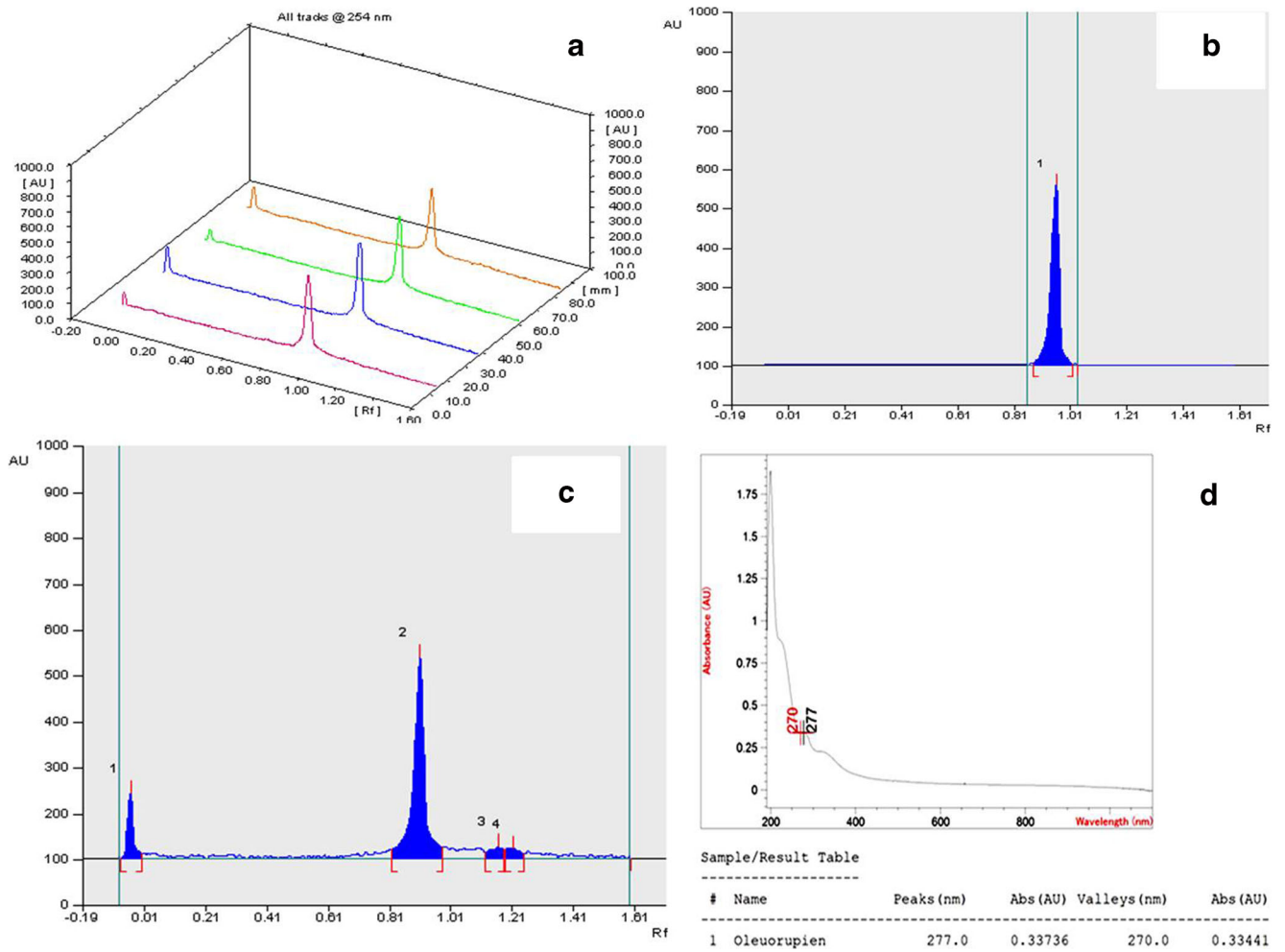| S.No | Methanolic Fractionates (%v/v) | % Oleuropein |
|------|------|------|
| 1 | 0 | 50.8 |
| 2 | 10 | 52.8 |
| 3 | 20 | 65.2 |
| 4 | 30 | 86.5 |
| 5 | 40 | 98.5 |
| 6 | 50 | 75.5 |
| 7 | 60 | 66.3 |
| 8 | 70 | 72.5 |
| 9 | 80 | 63.5 |
| 10 | 90 | 61.5 |
| 11 | 100 | 76.8 |

Fig. 1  **a** HPTLC Linearity tracks of Oleuropein recorded at 254 nm; **b** HPTLC Chromatogram for Oleuropein Standard; **c** HPTLC Chromatogram for Fractionate; (D) Overlaid spectrum of Olive leaf Extract 4

Fig. 2  Comparative DSC Thermograms of (**a**) Oleuropein Extract (**b**) Physical Mixture − 1 (Oleuropein: Tefose, Capmul, in a ratio of 10:5:5) (**c**) Physical Mixture −2 (Oleuropein: Tefose, Capmul, Polaxomer 188, Tween 80 in a ratio of 10:5:5:5:5); (**d**) Thermal peak of Oleuropein loaded NLC
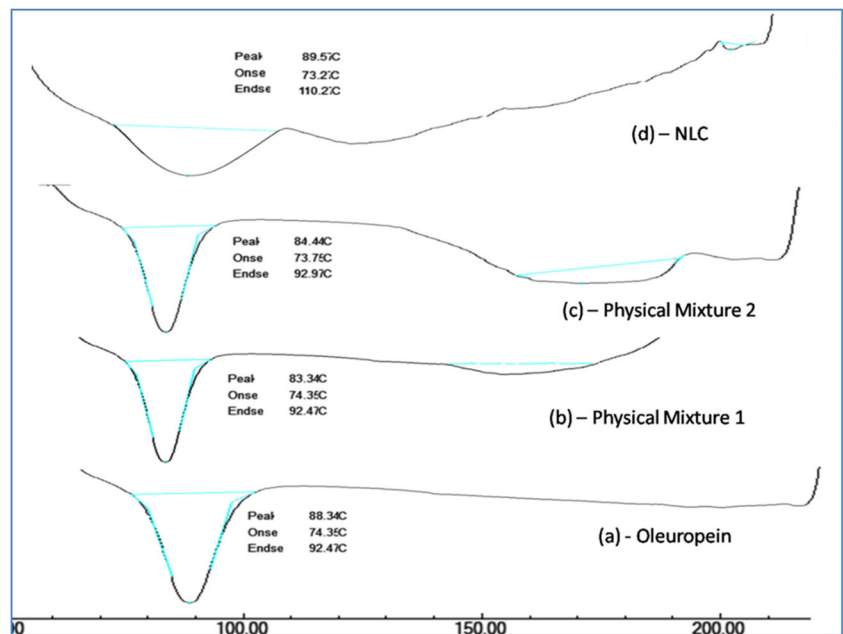
particle size and large surface area of NLC leads to decrease in crystallization point. The CI % of drug and bulk lipid NLC was found to be 100% and 15% indicating the complete crystallization of lipid after production. According to Siekmann and Westesen (1994), the decrease in the melting point of NLC is due to their large surface to volume ratio and rapid crystallization of lipid matrices.

## Experimental design

The result of experimental design depicts that, the selected CMA's and CPP's shown significant effect on the CPS's. It provides considerable useful information and reaffirms the utility of statistical design for the conduct of experiments. The statistical interpretation of the data was tabulated in Tables 2 and 3 which suggests that the model was fitted to data and it was significant at $p$ value <0.05. These findings were based on F-test, $p$ value at 95% CI, co-efficient of determination. The results ascertained a good value of coefficient of determination with $R^2 = 94\%$ for particle size, $R^2 = 88\%$ for zeta potential and $R^2 = 82\%$ for entrapment efficiency. Hence, desired model was chosen based on the selection criteria of p < f value. Low SD, lower predicted residual error sum of squares, high $R^2$ value. Lack of fit values for the responses, PS is 0.1197, ZP is 0.0751 and EE is 0.7710 (P > F value). Hence, it was not significant (P Value >0.05) which indicates that data can be well explanatory by using regression model. Fit summary statistics were given in Table 4 and for the responses PS, ZP and EE, P value was estimated by F-test in ANOVA and the results are presented

in Table 5. In general, $P$ value less than 0.05 indicates, the terms are significant enough to show interactions on the responses. The regression equation reflects that almost 95% of the experiment can be well fitted to the model selected. Hence the model is navigated to predict the design space.

## Effect of CQAs and CPP's on particle size

The particle size of the formulation was range between 169.5 and 480.0 nm. The statistical analysis of the executed design suggest that, the proposed model was significant ($P < 0.05$) and it ends with a high and pretty good coefficient of determination ($R^2 = 94\%$). Lack of fit (P > F) indicates that higher order interaction are not important and residuals are distributed randomly which ensures the appropriateness of the mathematical model. Probability plot represents a straight line with represents normal distribution of residuals. Among the factors, concentration of liquid lipid ($X_1$), Homogenization time ($X_3$), Interaction effects concentration of liquid lipid and homogenization time ($X_1$, $X_3$) shows significant effect on the PS. The regression equation for PS in terms of factors is derived as follows.

$$Y_1 = 223.1 + 75.5\,X_1 + 1.962\,X_2 + 24.3\,X_3 - 4.54\,X_1X_2$$
$$+ 58.31\,X_1X_3 + 2.54\,X_2X_3 + 19.6\,X_1{}^2$$
$$+ 9.81\,X_2{}^2 - 3.87\,X_3{}^2$$

The main effects $X_1, X_3$ and interaction effect $X_1X_3$ shows +ve synergistic effect on the response. From the regression

**Table 2** Central Composite Experimental design consisting of experiments for the study of CMA's and CPP's on CQA's represented in actual values with experimental results

| Formulation Run | Conc.of Liquid Lipid (%w/w) | Conc. of Surfactant (%w/v) | Homogenization Time (Min) | Particle Size (nm) | Zeta Potential (mV) | Entrapment Efficiency (%) |
|---|---|---|---|---|---|---|
| F1 | 4 | 2 | 15 | 383.8 ± 2.22 | −14.6 ± 1.20 | 68.6 ± 3.12 |
| F2 | 3 | 0.977311 | 15 | 293.7 ± 2.20 | −11.3 ± 1.22 | 84.4 ± 4.24 |
| F3 | 2 | 3 | 10 | 194.4 ± 2.18 | −19.9 ± 1.24 | 89.8 ± 3.16 |
| F4 | 3 | 5 | 20 | 239.6 ± 2.04 | −15.3 ± 1.32 | 88.6 ± 3.24 |
| F5 | 2 | 5 | 20 | 170.7 ± 2.42 | −24.3 ± 1.12 | 80.6 ± 3.34 |
| F6 | 2 | 2 | 20 | 169.5 ± 2.12 | −27.1 ± 1.20 | 98.4 ± 4.24 |
| F7 | 3 | 6.022689 | 15 | 251.9 ± 2.14 | −12.8 ± 1.42 | 84.4 ± 4.46 |
| F8 | 3 | 3.5 | 15 | 216.0 ± 2.22 | −18.8 ± 1.24 | 90.5 ± 3.46 |
| F9 | 4.681793 | 3.5 | 15 | 479.9 ± 2.42 | −16.6 ± 1.20 | 80.6 ± 3.20 |
| F10 | 3 | 3.5 | 6.591036 | 191.6 ± 2.24 | −20.7 ± 1.24 | 92.3 ± 4.24 |
| F11 | 1.318207 | 3.5 | 15 | 196.8 ± 2.20 | −18.3 ± 1.34 | 91.6 ± 4.32 |
| F12 | 3 | 3.5 | 15 | 223.1 ± 2.12 | −18.8 ± 1.36 | 83.3 ± 3.24 |
| F13 | 3 | 3.5 | 15 | 221.0 ± 2.42 | −17.2 ± 1.48 | 94.6 ± 3.16 |
| F14 | 4 | 2 | 20 | 422.0 ± 2.64 | −11.7 ± 1.52 | 80.5 ± 3.26 |
| F15 | 2 | 5 | 10 | 189.4 ± 2.74 | −14.5 ± 1.80 | 82.5 ± 4.18 |
| F16 | 3 | 3.5 | 23.40896 | 236.6 ± 2.84 | −23.0 ± 1.42 | 87.2 ± 4.34 |
| F17 | 4 | 5 | 10 | 236.9 ± 2.34 | −15.5 ± 1.36 | 92.5 ± 3.18 |

**Table 3** The Quantitative Factor effects and associated *p* Value for each response

| Parameter | Particle Size (Y1) | | ZP (Y2) | | % EE (Y3) | |
|---|---|---|---|---|---|---|
| | Coefficient | *p* value | Coefficient | *p* value | Coefficient | *p* value |
| Intercept | 223.17 | 0.000 | −18.10 | <0.0001 | 88.8 | <0.0001 |
| X1 | 75.595 | <0.220 | **1.695** | **0.021** | **−3.05** | **0.050** |
| X1$^2$ | 19.611 | 0.081 | 0.038 | 0.952 | −1.335 | 0.380 |
| X2 | 1.962 | 0.840 | 0.610 | 0.344 | 0.655 | 0.652 |
| X2$^2$ | 9.815 | 0.347 | **1.973** | **0.015** | −1.666 | 0.283 |
| X3 | **24.330** | **0.041** | −0.508 | 0.442 | 0.352 | 0.819 |
| X3$^2$ | −3.878 | 0.695 | **−1.367** | **0.059** | 0.401 | 0.785 |
| X1X2 | −4.54 | 0.780 | −0.497 | 0.635 | **8.235** | **0.009** |
| X1X3 | **58.31** | **0.008** | **2.948** | **0.022** | 0.357 | 0.886 |
| X2X3 | 2.541 | 0.867 | −0.200 | 0.836 | −1.832 | 0.424 |
| $_R2$ | 0.9374 | | 0.9682 | | 0.8254 | |
| R$^2$(Adj.) | 0.8571 | | 0.9022 | | 0.9120 | |

Bold Entries implies that a particular main effects, interaction and quadratic effects were significantly affecting the responses

polynomial equation, it was ascertained that the concentration of liquid lipid and HT shows +ve effect on PS i.e., Increase in the liquid lipid concentration n enhances the saturation solubility of drug; thereby it reduces the Crystallinity and enhances micellar solubilization. Increase in homogenization time will enhance the capillary forces between the particles, leads to cavitation's of globules and ends with fine narrow particles of minimal particle size. Increase in the concentration of solid lipid results in increased viscosity of dispersion, leads to higher surface tension and hence large Particle size was obtained. The large *P* value for lack of fit indicates that, lack of fit is insignificant; it explores a significant model correlation between the factors and responses.

### Effect of CMA's and CPP's on zeta potential

The Zeta potential of the formulation was range between −11.32 and −27.1 mV. The CMA's, concentration of surfactant and concentration of Liquid lipid and CPP's,

homogenization time shows a significant effect on response, zeta potential. From the fit summary data as shown in Table 3, it was observed that two way interaction effects and quadratic effects shows predominant effect on the response (Zeta potential). A significance was predicted at 'P' 0.05% and lack of fit is 0.0751 (P > F). Hence the model is significant enough to predict the interactions between CMA's, CPP's with CQA. The R$^2$ square value is 0.88 i.e., 88% of total variations are explained by this model. The polynomial equation of the fitted model constructed for response ZP was presented below.

$$Y_2 = -18.1 + 1.695\ X_1 + 0.61\ X2 - 0.508859\ X_3$$
$$+ -0.497\ X_1\ X_3 + 2.94\ X_1\ X_3 - 0.200\ X_2\ X_3$$
$$+ 0.038\ X_1{}^2 + 1.97\ X_2{}^2 - 1.36\ X_3{}^2$$

The model involves quadratic effects and curvature of response plot shows that, RSM (CCRD) is a best chosen experimental design or the data. From the equation, $X_2{}^2$ and $X_1$ and

**Table 4** Fit Summary Statistics for Particle size, Polydispersibility Index and Entrapment Efficiency by ANOVA

| Response | Source | DF | Sum of squares | Mean of squares | F | Fcritic |
|---|---|---|---|---|---|---|
| Y1 | Model | 9 | 100,965.25 | 11,218.4 | 11.6564 | 3.6766 |
| | Error | 7 | 6736.93 | 962.4 | | |
| | Cumulative total | 16 | 107,702.18 | | | |
| Y2 | Model | 9 | 201.63 | 22.40 | 5.6919 | 3.6766 |
| | Error | 7 | 27.55 | 3.93 | | |
| | Cumulative total | 16 | 229.18 | | | |
| Y3 | Model | 9 | 648.82 | 72.09 | 3.4347 | 3.6766 |
| | Error | 7 | 146.92 | 20.98 | | |
| | Cumulative total | 16 | 795.74 | | | |

**Table 5** Comparative In-vivo Pharmacokinetic Studies data for Oleuropein and Oleuropein loaded NLC administered through IV and IN Route

| Parameter | Unit | Oleuropein | Oleuropein NLC (Insitu gel) | |
|---|---|---|---|---|
| | | Extra vascular administration (Plasma Concentration) | IV Administration (BrainConcentration) [a] | IN Administration (BrainConcentration) [b] |
| t1/2ka | Min | 0.58103772 | – | – |
| t1/2k10 | Min | 1.180639353 | 3.76978613 | 5.4347 |
| V/F | (mg)/(mg/ml) | 18.37971308 | 2.462380734 | 0.182999079 |
| CL/F | (mg)/(mg/ml)/min | 10.79063329 | 0.123951981 | 0.0595227 |
| Tmax | Hrs | 1.170245356 | – | 23 |
| Cmax | mg/ml | 0.273704196 | 2.4 | 7.300366649 |
| Css | mg/ml | – | – | 7.30445 |
| AUC 0-t | mg/ml*min | 0.926729668 | 68.07493555 | 151.790 |
| AUC 0-inf | mg/ml*min | 0.926729668 | 80.67640346 | 168.00 |
| MRT | Hrs | 2.541562777 | 19.56 | 23.15 |

Compared with control group

[a] $P < 0.05$; Compared with control group and negative control

[b] $P < 0.05$ (IV was compared with control and IN was compared with both control and negative control)

$X_1 X_3$ shows positive effect on the ZP i.e., increase in concentration of surfactant enhances the zeta potential and homogenization time shown significant negative effect on ZP. The effect is ascertained due to the surface charge modification of drug on the lipid matrix and its encapsulation results in surface charge stabilize and increase the ZP. Homogenization, results is reduced PS, thereby it causes upswing in surface free energy which imparts some inverse effect on ZP.

## Effect of CMA's and CPP's on %EE

The entrapment efficiency the formulation was range between 68.6 and 98.4%. The statistical interpretation of the executed design depicts that the two way interactions between, concentration of liquid lipid and concentration of surfactant ($X_1X_2$) and main effect concentration of liquid lipid shows a significant effect on entrapment efficiency. The linear regression shows a good co-efficient of determination ($R^2 = 0.82$) i.e., 82% of interactions are well executed by this model. Lack of fit (p > F) indicates quadratic interaction are not important and residuals are distributed randomly which ensures appropriateness of the model. The regression equation for encapsulation efficiency is

$$Y_3 = 88.8 - 3.05X_1 + 0.65X_2 + 0.3X_3 + 8.23X_1X_2$$
$$+ 0.357X_2X_3 - 1.832X_2X_3 - 1.33X_1{}^2 - 1.66X_2{}^2$$
$$+ 0.401X_3{}^2$$

$X_1X_2$ shows positive effect on the entrapment efficiency whereas $X_1$ shows negative effect on the entrapment efficiency, increase in the concentration of liquid lipid decreases the entrapment efficiency due to leakage of drug from the lipid matrix and increase in concentration of surfactant enhances entrapment efficiency which is attributed due to reduced surface tension, enhanced micellar solubilization and increased contact of drug with lipids. Predicted and observed values of response shows good correlation, hence the model is good enough to navigate the deign space.

## Data optimization and method validation

2D Contour and 3D response plots were mentioned in Fig. 3. Graphical optimization was done by superimposing the critical response plots on a contour plot. Magnitude of error is useful to establish the reliability of generated equation and to express relevant domain of model. After generating the regression polynomial equation the formulation was optimized for three CQA's by using maximum desirability function of response like PS, ZP and EE. The composition of optimal formulation was 2.94% of liquid lipid, 2.5% of surfactant and 19.8 min of homogenization time using Micro emulsification – ultrasonication method. At these levels the predicted values of $Y_1, Y_2$ and $Y_3$ are $177.8 \pm 2.54$ nm, $-22.5 \pm 1.46$ mV and $90 \pm 2.6$% EE respectively. The observed responses are $177.5 \pm 2.64$ nm, $-21.8 \pm 2.12$ mV and $89 \pm 2.66$% EE respectively. A comparison between the predicted and observed responses shows a good correlation which ascertains the reliability of CCRD in predicting desirable NLC formulation.

SEM and TEM images were given in Fig. 4. The images exhibits spherical shaped particles with irregular surface.
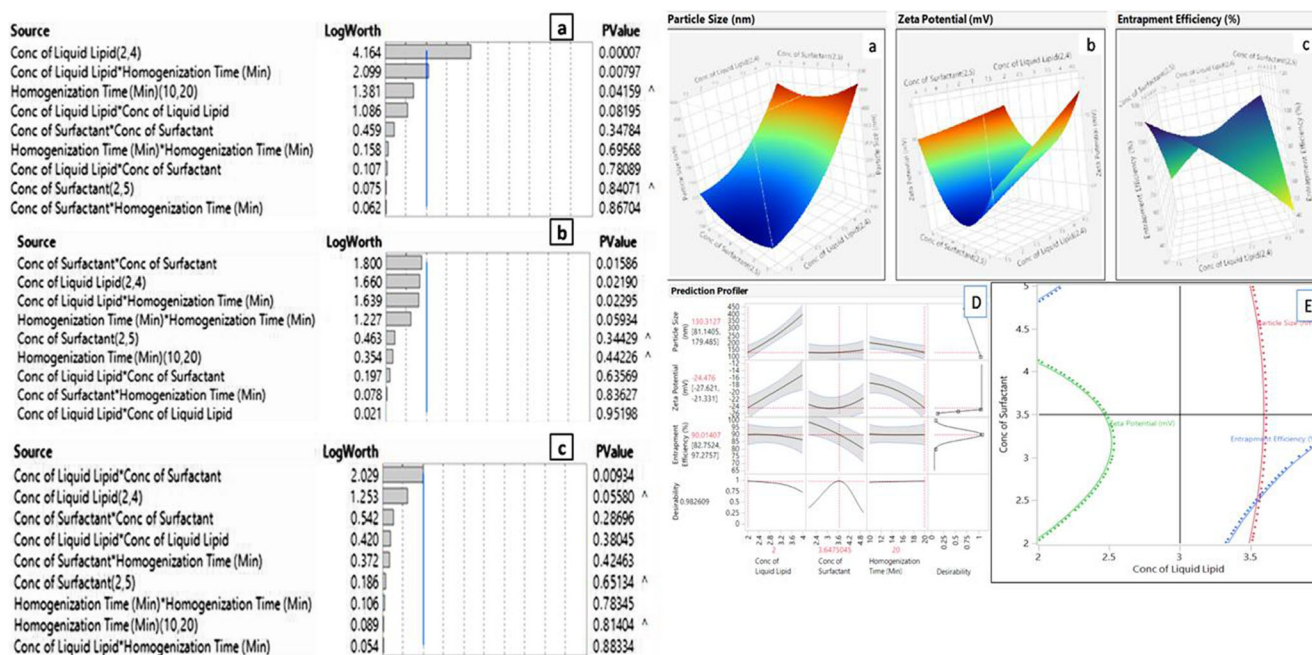
**Fig. 3** Pareto Chart and Response surface plots for the effect of CMA and CPP on **a** Particle Size in nm; **b** Zeta potential in mV; **c** Entrapment efficiency in %; **d** Prediction profiler plots representing maximum desirability of CMA and CPP; **e** Contour plot representing synergistic and antagonistic effect of CMAs and CPPs on CQA

## Determination of nanoparticle induced hemolysis

From the data, it was observed that there was no notable lysis of erythrocytes after administration of drug loaded NLC. Hence, there is no sign of toxicity with the designed formulation. In general, haemolysis of cells causes jaundice, Anemia and other blood related problems. During the study, haemolysis of cells releases hemoglobin which was oxidized into methehemoglobin by ferricyanide in the presence of bicarbonates. Finally methemoglobin was transferred into cyanomethmoglobin by cyanide. The hemoglobin % was almost 1% and it indicated haemocompatibility of OLE loaded NLC with blood components.

## Invivo nasal toxicity evaluation

Anterior cross section of nasal cavity was used for examination. Studies were performed to identify the toxicity of excipients used in the formulation. Histopathological results were reflected in the Fig. 5 and the results shows that after intranasal administration of NLC for 15 consecutive days, nasal mucosa conferred as –ve control does not exhibit any mucociliary damage and epidermal linings were intact. Specimens conferred as +ve control manifests shrinkage and detachment of nasal cilia. Blank NLC and OLE NLC do not exhibits significant changes in the morphology of nasal cilliary epithelium due to encapsulation of drug which reduces the direct irritant effect on nasal tissue. Hence, NLC are safer for administration of drug through nasal route.

## Invitro drug release studies

Invitro drug release studies were mentioned in Fig. 6a which depicts that OLE NLC shows burst effect followed by prolonged effect for 24 h and the % drug released was found to be 95%. Release of OLE from NLC was more consistent in relevance to plain drug solution. The narrow PDI, conc. of surfactant enhances the wettability and solubilization of drug which aids in formation of pores in the matrix. This nails a predominant role in the consistent release of drug from OLE NLC. From the Invitro kinetic models, it was noted that OLE NLC follows first order kinetics.

## In-vivo pharmacokinetic study

The PK parameters were mentioned in the Table 5 and Invivo drug release patterns were shown in Fig. 6b. The concentration of drug in blood and brain was estimated upto 6 h using a validated HPLC method. Oleuropein solution has high plasma concentration upon administration through IV route in comparison to IN route. The higher systematic concentration of drug may be due to inability of drug to cross BBB because of its hydrophilic nature through passive diffusion. The peak plasma concentration of drug after the administration of Oleuropein NLC (IN) was found to be 7.300 mg/ml within 2 h respectively. In intranasal route, the availability of drug in SC is expected due to systemic absorption of drug and reduced mucocilliary clearance from nasal mucosa. NLC formulation attains a notable higher half-life in brain and plasma
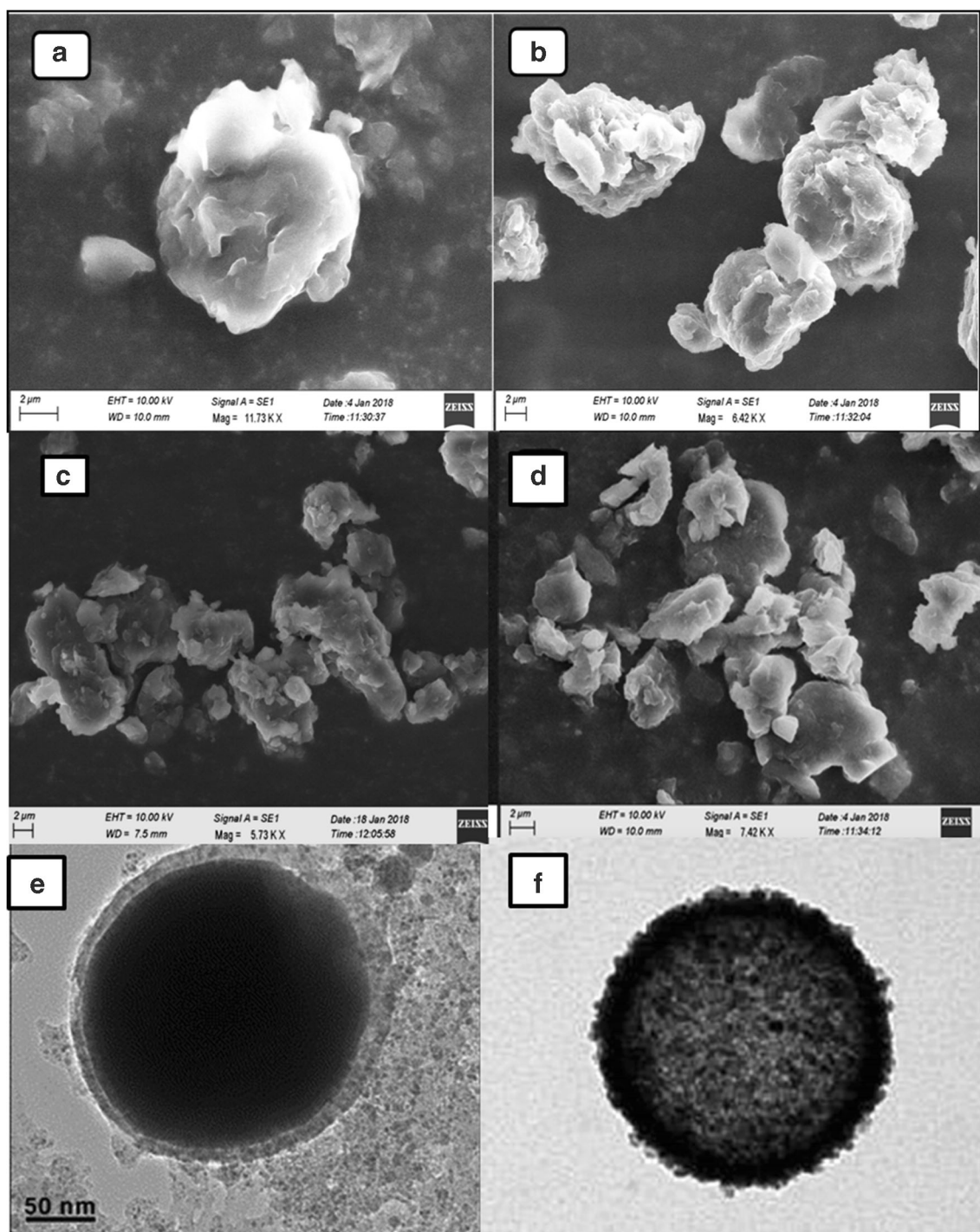
**Fig. 4** SEM and TEM Studies of optimized NLC (F9) with entrapped drug; (**a**) SEM Images of Single Nanostructured Lipid carrier at 100X; (**b**) Chain like Nanostructured Lipid carrier; (**c**) Group of Nanostructured Lipid carrier; (**d**) Blocks like Nanostructured lipid carrier, (**e**) TEM image showing the lipid encapsulation; (**f**) TEM image showing the drug encapsulated in NLC

compared to OLE-solution with slow rate of elinmation (Ke). The brain concentration of OLE was significantly high in Oleuropein NLC which was administered in both IV and IN route upto 6 h. This was attributed due to longer residence time of drug in rat nasal cavity which promoted absorption of drug and provides an opportunity for systemic sustained drug delivery to brain. During early first hour, the systemic concentration of drug was not significant enough to achieve therapeutic activity. This observed was ascertained due to slower release of drug from lipid matrix. The bioavailability
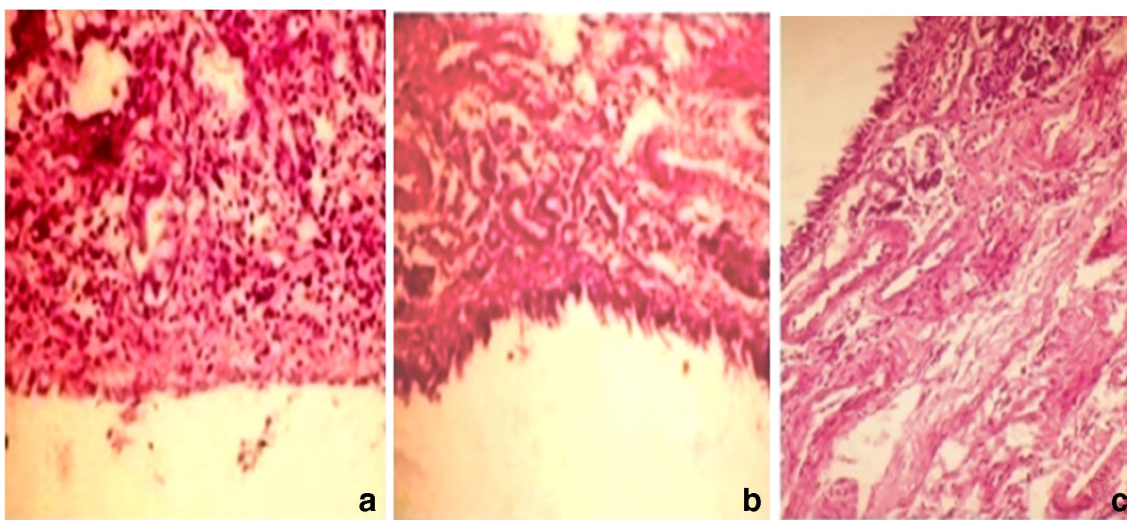
**Fig. 5** Histo-pathological images of nasal mucosa focused at a magnification of 100X representing (**a**) Untreated Nasal epithelium showing Normal intact surface of mucosa; (**b**) Nasal epithelium treated with Oleuropein showing focal inflammatory cells in lamina propria of mucosal lining; (**c**) Nasal epithelium treated with Oleuropein Loaded NLC showing diffuse inflammatory cells infiltration in lamina propria of destructed mucosal lining epithelium

of Oleuropein –NLC was high in IN route compared to IV route. This enhanced absorption of OLE from OLE-NLC was due to small size, lipid mature of NLC, protection of drug from metabolic enzymes and epithelial cells lining the cavity. The NLC underwent transcellular pathway through olfactory neurons to brain via endocytic pathways. These observations

**Fig. 6** (**a**) Comparative Invitro drug release studies between Oleuropein and Oleuropein Loaded NLC (**b**) In-Vivo Pharmacokinetic profiles of Oleuropein, Oleuropein NLC optimized formulation in plasma of Wistar rats which is administered through IV and IN routes
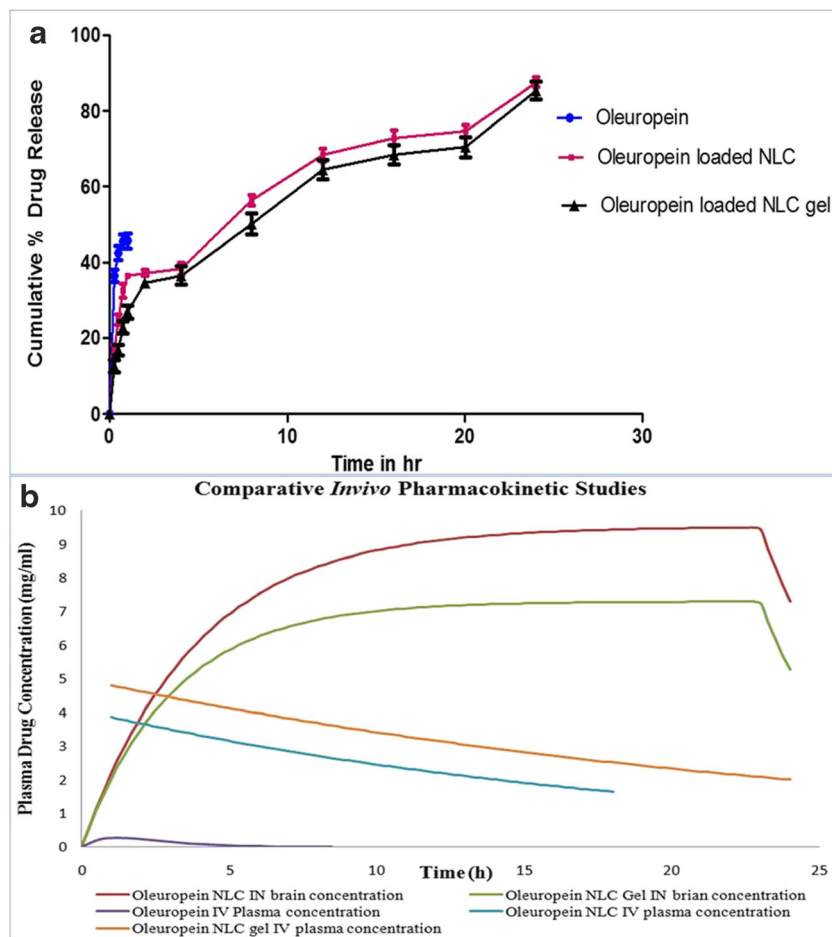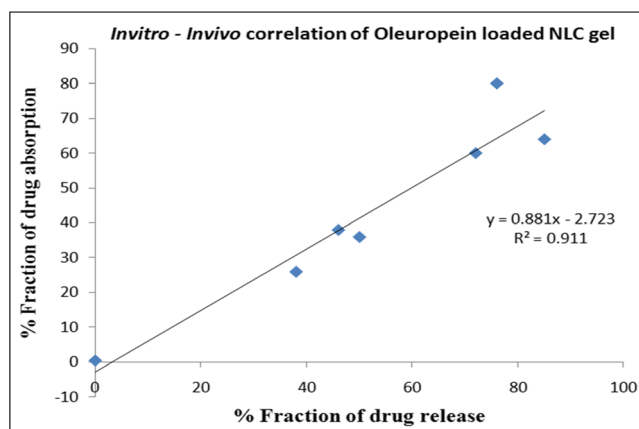
**Fig. 7** Invitro – Invivo correlation of Oleuropein Loaded NLC

are well correlated with the findings done by seju et.al. Brain to blood ratio was also calculated for all the formulation to estimated targeting efficacy of NLC.DTP % and DTE % was assured to predict the direct transport of drug from nose to brain via olfactory pathway. OLE NLC (IN) shows highest DTP % of 83.07% which indicates NLC improves brain targeting efficiency compared to solution in IN route. Higher DTE % of OLE loaded NLC was resulted due to reduced clearance, high permeation of drug through nasal mucosa by olfactory pathway into brain. The drug is releasing from NLC by diffusion, and undergo transcellular pathway which transport the drug into olfactory bulb and brain stem finally reaching CSF. For intra-axonal or intra mucosanal transport, the particle size of NLC should be less than 100 nm. In transcellular pathway, NLC can be navigated through epithelial cells and reach lamina propia, After that, they may absorb into systemic circulation can absorb into cervical lymph nodes of neck or and undergo extravascular diffusion through perineural and perivascular spaces which ends up with entry of NLC into cranial compartment. This observation proves that, the drug oleuropein was transporting directly into CNS after IN delivery of NLC. Hence, NLC is a powerful colloidal carrier for brain targeting of hydrophilic molecules through intranasal route.

## Invitro – Invivo correlation studies

Level A, point to point correlation between Invitro dissolution and Invivo absorption was done using wagnor-nelson method and the percentage absorption data vs. percentage drug release was shown in Fig. 7. NLC exhibits higher percentage of absorption and both profiles are joined at a single point in 23 h. plotting a fraction of drug absorbed against fraction of drug release from the NLC shows a linear correlation with $R^2$ values of 0.911 indicating that the Invitro release profile can be used to predict the Invivo performance of drug loaded NLC.

## Conclusions

In the present research, we successfully designed a robust, novel and herbal nanocarrier based on lipid and polymer for nasal delivery of Oleuropein. QbD approach enables us to identify critical material and process attributes influencing PS, ZP & EE. Design Space was generated using Central Composite Design from which PS and ZP was measured by Dynamic Light Scattering technique. The optimized batch (F9) was formulated by selecting the points with in design space which shown a minimal PS 169 nm, ZP −27 mV with entrapment efficiency of 98.4% and narrow particle size distribution. SEM & TEM analysis projects spherical shaped particles with smoother surface morphology. Thermal studies demonstrated that crystalline peaks were disappeared in Oleuropein NLC which prevails higher incorporation of drug in NLC. Nasal permeation studies depicts a higher permeation of drug from NLC through nasal mucosa due to its minimal particle size and enhanced surface area for diffusion compared to oleuropein solution. Histo-Pathological studies prove safety of NLC for IN administration. In-Vitro drug release profile exhibit initial burst release followed by sustained release consequently for 24 h. In-vivo pharmacokinetic studies reveal that IN route is a potential non-invasive method for brain targeting of hydrophilic drug compared to IV and loading of drug into NLC encounters the challenges of permeation of drug through BBB. Based on the findings from molecular, physicochemical and pre-clinical aspects, the designed nanocarrier made of Tefose and Capmul possesses the potential to entangle the drug Oleuropein in brain through nasal route which declines the dose and dosing frequency, attains prolonged release of drug to manifest sustainable action. In a nutshell, the current research opens new horizons for delivery of hydrophilic drugs to brain through transnasal flux.

## Compliance with ethical standards

**Conflict of interest** All authors declare no conflict of interest.

**Ethical approval** This article does not contain any studies with human participants.

# References

1. Hailong Y, Liu P, Tang H, Xiang JJ, Chen L. Oleuropein, a natural extract from plants, offers neuroprotection in focal cerebral ischemia/reperfusion injury in mice. Eur J Pharmacol. 2016;775: 113–9. https://doi.org/10.1016/j.ejphar.2016.02.027.

2. Alam I, Baboota S, Ahuja A, Ali M, Ali J. Intranasal administration of nanostructured lipid carriers containing CNS acting drug: Pharmacodynamic studies and estimation in blood and brain. J Psychiatr Res. 2012;46:1133–8. https://doi.org/10.1016/j.jpsychires.2012.05.014.

3. Beloqui, Solinics MA, Delgado A, Evora C, Pozo Roodruguez A. Bio-distribution of nanostructured lipid carriers after intravenous administration to rats: influence of technological factors. Eur J Pharm Biopharm. 2013;84:309–14. https://doi.org/10.1016/j.ejpb.2013.01.029.

4. Doktorovova S, Souto E, Silva A. Nanotoxicology applied to solid lipid nanoparticles and nanostructured lipid carriers- a systematic review of in-vitro data. Eur J Pharm Biopharm. 2014;87:1–18. https://doi.org/10.1016/j.ejpb.2014.02.005.

5. Beloqui A, Solinis MA, Rodriguez A, Antonio V. Nanostructured lipid carriers: promising drug delivery systems for future clinics. Nanomedicine. 2016;12:143–61. https://doi.org/10.1016/j.nano.2015.09.004.

6. Zhang X, Liu J, Liu H, Ni J, Zhang W, Shi Y. Formulation optimization of dihydroartemisinin nanostructured lipid carrier using response surface methodology. Powder Technol. 2010;197:120–8. https://doi.org/10.1016/j.powtec.2009.09.004.

7. Yateem H, Afaneh I, Al-Rimawi F. Optimum conditions for oleuropein extraction from olive leaves. Int J Appl Sci Technol. 2014;4:153–9.

8. Rios F, Gutiérrez-Rosales F. Comparison of methods extracting phenolic compounds from lyophilised and fresh olive pulp. Food Sci Technol. 2010;43:1285–8.

9. Kovacevic A, Savic S, Vuleta G, Muller RH, Keck CM. Polyhydroxy surfactants for the formulation of lipid nanoparticles: effect on size, physical stability and particle matrix structure. Int J Pharm. 2011;406: 163–72. https://doi.org/10.1016/j.ijpharm.2010.12.036.

10. Gaba YM, Kamel AO, Sammour OA, Elshafeey AH. Effect of surface charge on the brain delivery of nanostructured lipid carrier's in situ gels via nasal route. Int J Pharm. 2014;473:4420–57. https://doi.org/10.1016/j.ijpharm.2014.07.025.

11. Dolatabadi JEN, Azami A, Mohammadi A, Hamishehkar H, Panahi-azar V, Saadat YR, et al. Formulation, characterization and cytotoxicity evaluation of Ketotifen loaded nanostructured lipid carriers. Journal of Drug Delivery Science and Technology. 2018;46:268–73. https://doi.org/10.1016/j.jddst.2018.05.017.

12. Pokharkar VB, Jolly MR, Kumbhar DD. Engineering of a hybrid polymer lipid nanocarrier for the nasal delivery of Tenofovir disoproxil fumarate: physicochemical, molecular, Microstructural and stability evaluation. Eur J Pharm Sci. 2015;71:99–111. https://doi.org/10.1016/j.ejps.2015.02.009.

13. Pokharkar V, Gadhe AP, Palla P. Efavirenz loaded nanostructured lipid carrier engineered for brain targeting through intranasal route: in-vivo pharmacokinetic and toxicity study. Biomed Pharmacother. 2017;94:150–64. https://doi.org/10.1016/j.biopha.2017.07.067.

14. Yostawonkul J, Surassmo S, Iempridee T, Pimtongo W, Suktham K, Sajomsang W, et al. Surface modification of nanostructured lipid carriers by oleoyl quaternized chitosan as a mucoadhesive nanocarrier. Colloids Surf B Biointerfaces. 2017;149:301–11. https://doi.org/10.1016/j.colsurfb.2016.09.049.

15. Yostawonkul J, Surassmo S, Iempridee T, Pimtongo W, Suktham K, Sajomsang W, et al. Surface modification of nanostructured lipid carriersby oleoyl quaternized chitosan as a mucoadhesive

16. Ray S, Sinai P, Laha B, Maiti S, Bhattacharyya UK, Nayak AK. Polysorbate 80 coated cross linked chitosan nanoparticles of Ropinirole hydrochloride for brain targeting. Journal of Drug Delivery Science and Technology. 2018;48:21–9. https://doi.org/10.1016/j.jddst.2018.08.016.

17. Gartziandia O, Herran E, Pedraz JL, Carro E, Igartua M, Hernandez RM. Chitosan coated nanostructured lipid carriers for brain delivery of proteins by intranasal administration. Colloids Surf B Biointerfaces. 2015;134:304–13. https://doi.org/10.1016/j.colsurfb.2015.06.054.

18. Salama HA, Mohmoud AA, Kamel AO, Hady MA, Award GAS. Phospholipids based colloidal Polaxomer nanocubic vesicles for brain targeting via the nasal route. Colloids Surf B Biointerfaces. 2012;100:146–54. https://doi.org/10.1016/j.colsurfb.2012.05.010.

19. Fabregas A, Sanchez-Hernandez N, Tico JR, Garccia Montoya E, Perez Lozano P, Sune Negre JM. A new optimized formulation of cationic solid lipid nanoparticles intended for gene delivery: development, characterization and DNA binding efficiency of TCERG 1 expression plasmid. Int J Pharm. 2014;473:270–9. https://doi.org/10.1016/j.ijpharm.2014.06.022.

20. Fachel FNS, Medeiros Neves B, Dal Pra M, Schuh RS, Veras KS, Bassani VL, et al. Box-Behnken design optimization of mucoadhesive chitosan coated nanoemulsions for rosmarinic acid nasal delivery-Invitro studies. Carbohydr Polym. 2018;199:572–82. https://doi.org/10.1016/j.carbpol.2018.07.054.

21. Kozlovskaya L, Abou-Kaoud M, Stepensky D. Quantitative analysis of drug delivery to the brain via nasal route. J Control Release. 2014;189:133–40.

22. Mohammadi A, Jafari SM, Assadpour E, Esfanjani AF. Nano-encapsulation of olive leaf phenolic compounds through WPC-pectin complexes and evaluating their release rate. Int J Biol Macromol. 2016;82:816–22. https://doi.org/10.1021/jf060033j.

23. Meng F, Asghar S, Wang Y, Jin X, Wang Z, Wang J. Design and evaluation of lipoprotein resembling curcumin encapsulated protein free nanostructured lipid carrier for brain targeting. Int J Pharm. 2016;506:46–56. https://doi.org/10.1016/j.ijpharm.2016.04.033.

24. Blasi P, Schoubben A, Romano GV, Giovagnoli S, Di Michele A. Lipid nanoparticles for brain targeting. Technological characterization. Colloids Surf B: Biointerfaces. 2013;110:130–7. https://doi.org/10.1016/j.colsurfb.2013.04.021.

25. Han F, Li S, Yin R, Liu H, Xu L. Effect of surfactants on the formulation and characterization of a new type of colloidal drug delivery system: nanostructured lipid carriers. Colloids and Surfaces A: Physicochem Eng Aspects. 2008;315:210–6. https://doi.org/10.1016/j.colsurfa.2007.08.005.

26. Devakar TB, Tekade AR, Khandelwal KR. Surface engineered nanostructured lipid carriers for efficient nose to brain delivery of ondansetron HCl using Delonix regia gum as natural mucoadhesive polymer. Colloids Surf B: Biointerfaces. 2014;122:143–50. https://doi.org/10.1016/j.colsurfb.2014.06.037.

27. Nafee N, Makled S, Boraie N. Nanostructured lipid carriers versus solid lipid nanoparticles for the potential treatment of pulmonary hypertension via nebulization. Eur J Pharm Sci. 2018;125:151–62. https://doi.org/10.1016/j.ejps.2018.10.003.

28. Witayaudom P, Klinkesorn U. Effect of surfactant concentration and solidification temperature on the characteristics and stability of nanostructured lipid carriers (NLC) prepared form rambutan kernel fat. J Colloid Interface Sci. 2017;505:1082–92. https://doi.org/10.1016/j.jcis.2017.07.008.